Results in Physics 14 (2019) 102497

Contents lists available at ScienceDirect

Results in Physics

journal homepage: www.elsevier.com/locate/rinp

VIS-NIR spectral and particles distribution of Au, Ag, Cu, Al and Ni nanoparticles synthesized in distilled water using laser ablation

Mas Ira Syafila Mohd Hilmi Tan[a,b], Ahmad Fairuz Omar[a,c,*], Marzaini Rashid[a], Uda Hashim[c]

[a] School of Physics, Universiti Sains Malaysia, 11800 Penang, Malaysia
[b] Faculty of Mechanical and Manufacturing Engineering, Universiti Malaysia Pahang, 26600 Pahang, Malaysia
[c] Institute of Nano Electronic Engineering, Universiti Malaysia Perlis, 01000 Perlis, Malaysia

ARTICLE INFO

Keywords:
Laser ablation
Metal nanoparticles
Spectroscopy

ABSTRACT

In this research, gold (Au), silver (Ag), copper (Cu), aluminium (Al) and nickel (Ni) nanoparticles have been prepared by laser ablation in distilled water using Q-switched Nd: YAG. Comparative analysis between 1064 nm and 532 nm laser wavelength in term of absorption spectra and particle size distribution is performed. The synthesized nanoparticles were characterized by visible (VIS) and near infrared (NIR) spectrometer and transmission electron microscopy (TEM). The effect of laser pulse energy and laser wavelength on the size distribution and absorbance spectrum of metal nanoparticles was studied. The absorption peak intensities of the nanoparticles increase at higher laser pulse energy. It is discovered that for all metals, 532 nm laser produced nanoparticles with higher absorption peak intensities than 1064 nm. The work also shows that there is no noticeable difference in the size of the nanoparticles produced at 532 and 1064 nm for the Ni and Cu metals. However, a considerable size difference can be seen for Au, Ag, and Al at the two laser wavelengths. Smaller Ag nanoparticles were produced by 1064 nm laser while smaller Au and Al nanoparticles were produced by 532 nm laser.

Introduction

Nanotechnology is the comprehension and control of matter at the nanoscale where unique phenomena enable novel application which can significantly affect society. It has been utilized in various application, for example, in information and communication, food technology, energy technology, as well as some medical product and medicines [51]. Nanoparticles are defined as particles with size in the range of 1–100 nm at least in one of the three dimensions. Due to this tiny size scale, they retain a massive surface area per unit volume, a high proportion of atoms in the surface and near surface layers, and the capability to exhibit quantum effects. Nanoparticles can exist in various forms, such as metals, metal oxides, semiconductors, polymers, carbon materials, organics or biological. They also have a great morphological diversity of shapes such as spheres, cylinders, disks, platelets, hollow spheres and tubes [19]. For the past few years, the synthesis of metal nanoparticles is an essential subject of research in modern material science. Synthesis and optical properties of metal nanoparticles are of main significance due to unique properties which are different from those of bulk metals [52]. It is known that the method of synthesis has great influence on size and shape of nanoparticles. Hence, many techniques have been used such as lithography, thermal decomposition and laser ablation. Pulsed laser ablation was widely used for many applications in the synthesis of nanostructured materials. In recent times, pulsed laser ablation was employed for preparation of several metals and semiconductor materials in different media such as vacuum [10], open air [6], high purity gas [7] and liquid [30].

Laser ablation is the operation of removing small amount of the material surface by irradiating it with a laser beam. Laser ablation in liquids (LAL) is an effective and general path to synthesize and fabricate nanocrystals. Laser ablation in deionised water has been used widely to produce metallic [14], bi-metallic [20] and tri-metallic [46] nanoparticles as well as metal oxides [41]. Advantages of laser production of nanoparticles in liquid is the high purity of the nanoparticles produced, special surface charge characteristics and easy preparation in comparison with chemical methods. Laser energy is applied to a solid surface in a solvent during the laser ablation process. The target absorbs energy from the laser, vaporizes and condenses into the solution as a suspension of metal nanoparticles. The released nanoparticles carry a positive electrical surface charge and therefore, no chemical stabilizer is needed for electrostatic stabilization by the surrounding medium [50]. These advantages make metal nanoparticles produced by LAL method

* Corresponding author at: School of Physics, Universiti Sains Malaysia, 11800 Penang, Malaysia.
E-mail address: fairuz_omar@usm.my (A.F. Omar).

https://doi.org/10.1016/j.rinp.2019.102497
Received 7 February 2019; Received in revised form 30 June 2019; Accepted 30 June 2019
Available online 04 July 2019

Table 1
Metal nanoparticles synthesis using pulsed laser ablation method.

Author	Metals	Liquid	Absorption λ_{max} (nm)	Absorption peak		Particle size (nm)	
				1064 nm	532 nm	1064 nm	532 nm
Habieb et al. [8]	Au	Double distilled water	518–522	Increase	Decrease	15	23
Shukri et al. [37]	Au	Distilled water	520	Decrease	Increase	19	12
Solati et al. [39]	Ag	Acetone	400–480	Increase	Decrease	17–32	13
Hamad et al. [9]	Au	Distilled water	520–530	Increase	Decrease	31	9
	Ag	Distilled water	405	–	No peak	29	-
Muniz-Miranda et al. [18]	Cu	Distilled water	620	Increase	Decrease	4–5	1–3
Singh and Soni [38]	Al	Distilled water	264	Decrease	Increase	21	25
Baladi and Mamoory [3]	Al	Ethanol	210	Increase	Decrease	40–50 (Smaller)	40–50
Shalichah and Khumaeni [36]	Ni	Distilled water	290	–	–	25	–

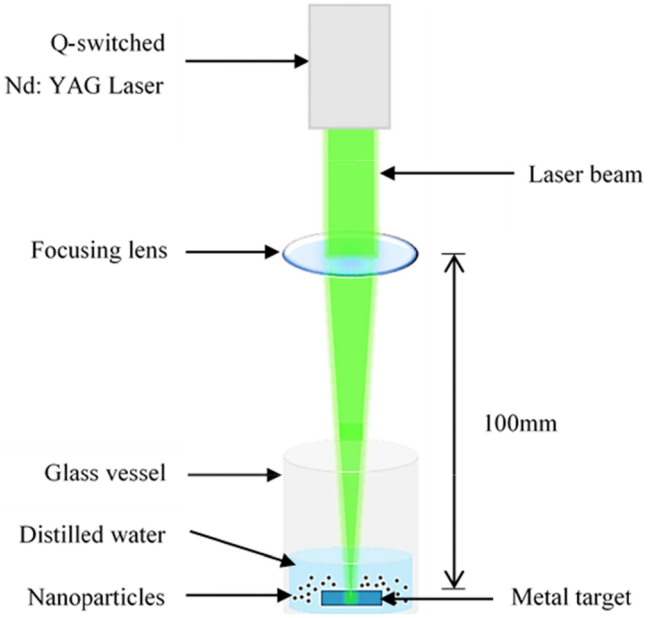

Fig 1. Schematic diagram of the pulsed LAL system.

exceptionally remarkable for several applications such as surface-enhanced Raman scattering (SERS), functional NPs for bio-applications, catalysis and energy-relevant applications [54]. All laser parameters are important in laser ablation process but the wavelength of laser has a special importance as the material's optical constants depend on wavelength. Metal nanoparticles and metal targets absorb the laser beam energy at the particular wavelength [33]. Thus, the ablation process will be affected by the choice of wavelength. The selected laser parameters also may be used to the size distribution and shape of the nanoparticles [38].

In recent years, there are still many ongoing researches on the application of laser ablation in synthesizing metal nanoparticles with the objective to control the particle shape, size and concentration in a variety of solution by controlling laser parameters such as laser wavelength, laser fluence and pulse duration [26]. Type of metal commonly used in synthesis includes gold [35,45,25], silver [6,39,53], copper [5,32,13], aluminium [48,40,11] and nickel [15], Muñetón Arboleda et al. [17,12]. The production of gold nanoparticles (AuNPs) has always receive major attention particularly on their synthesis-functionalization due to their broad application such as in chemical and biological sensing as well as in medical diagnosis and therapy. This leads to the publication of a number of review articles exclusively focusing on synthesis, characterization and application of gold nanoparticles [28,21,49]. Silver nanoparticles (AgNPs) on the other hand are known for their high electrical and thermal conductivity besides presenting antibacterial effects, high catalytic activity and important optical properties [16]. Copper nanoparticles (CuNPs) and Aluminium

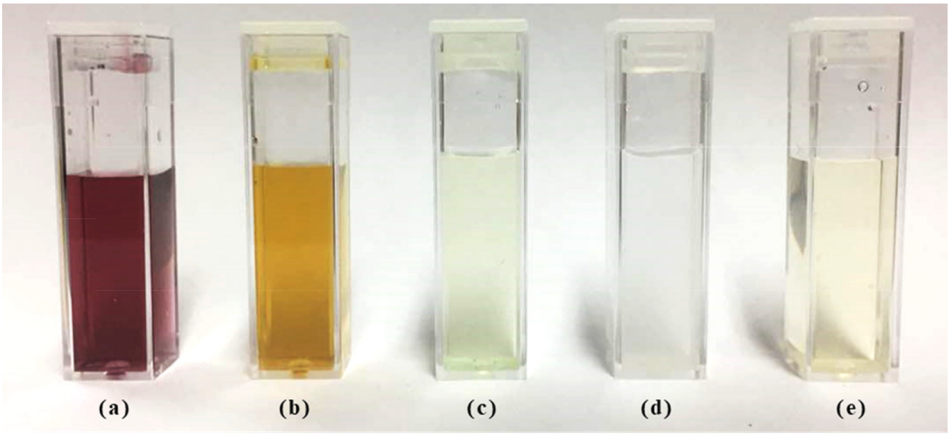

Fig. 2. Nanoparticles in distilled water by pulsed LAL; (a) AuNPs (b) AgNPs (c) CuNPs (d) AlNPs and (e) NiNPs.

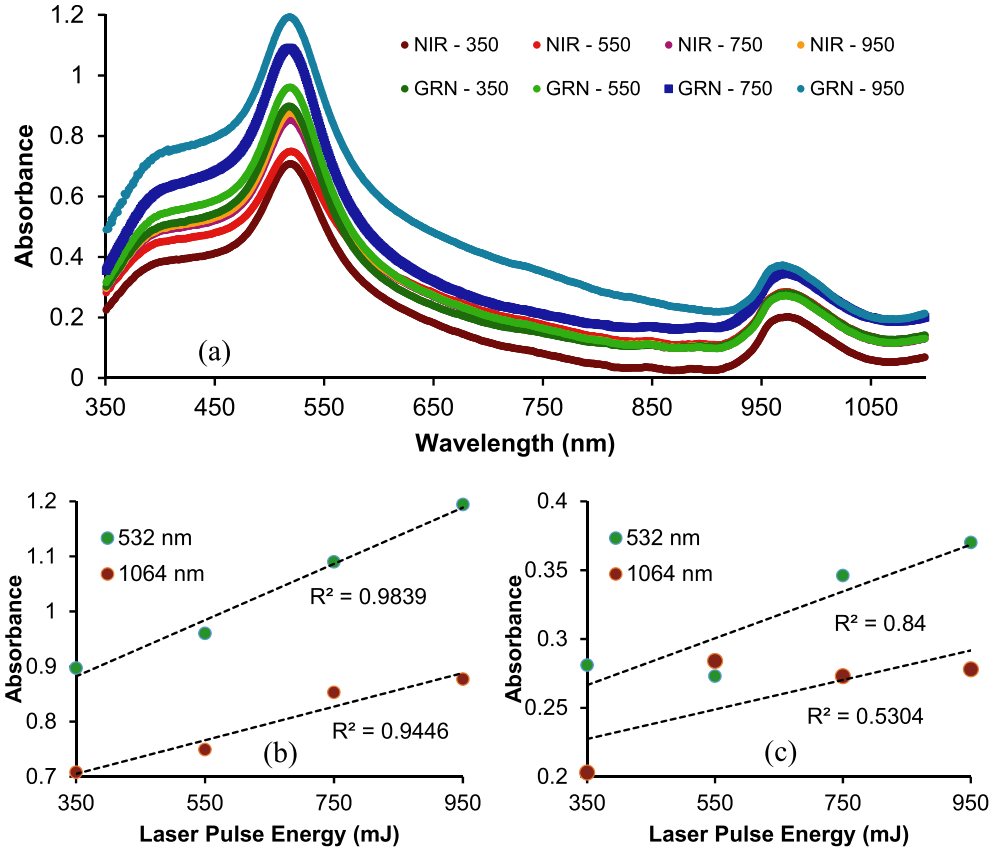

Fig. 3. (a) Absorption spectra of the synthesized AuNPs by different NIR (1064 nm) and green (532 nm) laser energies. Linear regression between absorbance and laser pulse energies measured using (b) peak visible spectra at 519.81 nm and 518.27 nm for AuNPs synthesized by 1064 nm and 532 nm laser respectively and (c) peak NIR spectra at 974.05 nm and 972.6 nm for AuNPs synthesized by 1064 nm and 532 nm laser respectively. (For interpretation of the references to color in this figure legend, the reader is referred to the web version of this article.)

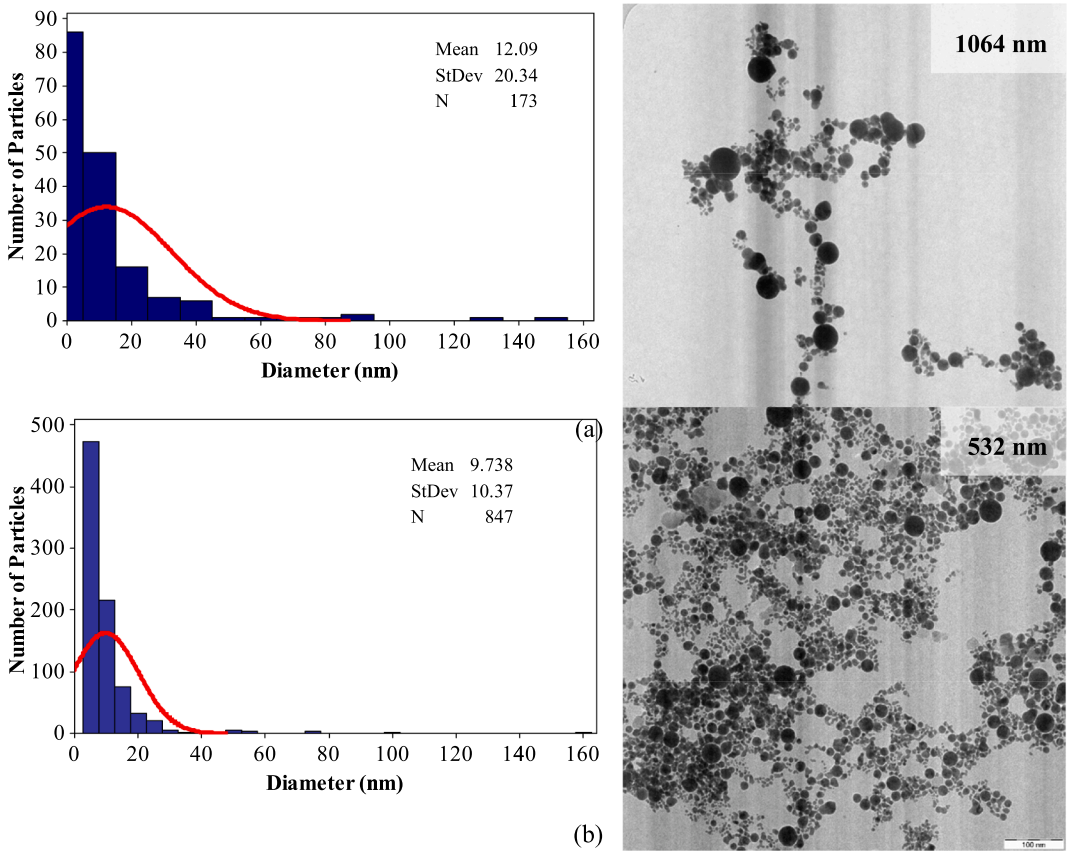

Fig. 4. Histogram of the size distribution and TEM images of the AuNPs produced by (a) 1064 nm and (b) 532 laser in distilled water.

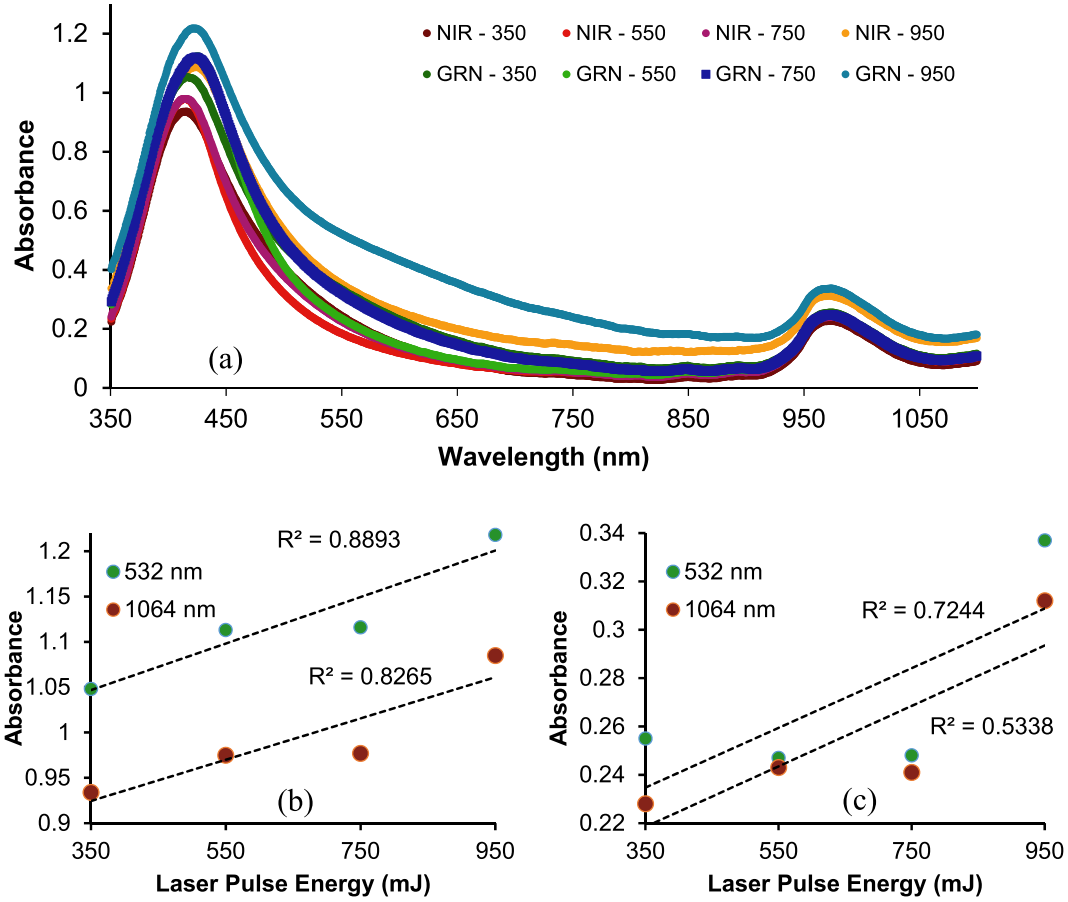

Fig. 5. (a) Absorption spectra of the synthesized AgNPs by different NIR (1064 nm) and green (532 nm) laser energies. Linear regression between absorbance and laser pulse energies measured using (b) peak visible spectra at 417.27 nm and 421.17 nm for AgNPs synthesized by 1064 nm and 532 nm laser respectively and (c) peak NIR spectra at 972.6 nm and 973.33 nm for AgNPs synthesized by 1064 nm and 532 nm laser respectively. (For interpretation of the references to color in this figure legend, the reader is referred to the web version of this article.)

nanoparticles (AlNPs) is gaining great attention among researchers as an alternative to noble metals due to their much lower cost, higher conductivity and ease of availability [26]. Optical, catalytical, mechanical and electrical properties of CuNPs allows them for a wide range of applications in the field of metallurgy, catalysis, nano and optoelectronics [42] while aluminium related materials has broad applications such as in fire retardant, catalyst, insulator, surface coating for corrosion resistant, composite materials and thermal protections such as in conductive and heat reflecting paints due to its properties such as high hardness, high stability, high insulation and transparency [27,4]. Nickel nanoparticles (NiNPs) on the other hand have shown their broad prospects in applications like conducting pastes, information storage, large-scale batteries, magnetic behavior, enhanced optical properties and biomedicine [17].

In this study, pulse laser ablations with two distinctive wavelengths (i.e. 532 nm and 1064 nm) and four different pulse energies (i.e. 350 mJ, 550 mJ, 750 mJ and 950 mJ) is used to synthesize various metals nanoparticles (i.e. AuNPs, AgNPs, CuNPs, AlNPs and NiNPs) in distilled water. The absorption spectrum and size distribution nanoparticles are characterized using VIS-NIR spectroscopy analysis and transmission electron microscopy (TEM) analysis. Table 1 lists the existing laser ablation results on related metal nanoparticles synthesized using 532 nm and 1064 nm laser wavelength. Regardless of numerous previous and ongoing studies on laser wavelength effects in production of nanoparticles, there are still no definitive conclusion that can be made. In most of the studies, the effect of laser wavelengths on the absorption spectra analysis and size distribution of nanoparticles produced noticeable differences. According to Resano-Garcia et al. [31], the major concern in the production of nanoparticles is to control the size distribution of the synthesized nanoparticles. Commonly, one of the techniques employed for optimization is by controlling the laser parameters such as its wavelength, pulse duration, energy, laser spot area, repetition rate and duration of experiment. However, the results between literatures may not easily be reproduced or compared due to different experimental conditions and potential interdependence of several processing parameters. Hence, the purpose of this research work is to compare the production of nanoparticles from various important metals under different laser parameters, but similar experimental setup.

Experimental methodology

Nanoparticles were synthesized by pulsed laser ablation using a Q-switched Nd:YAG (Neodymium-doped yttrium aluminum garnet;

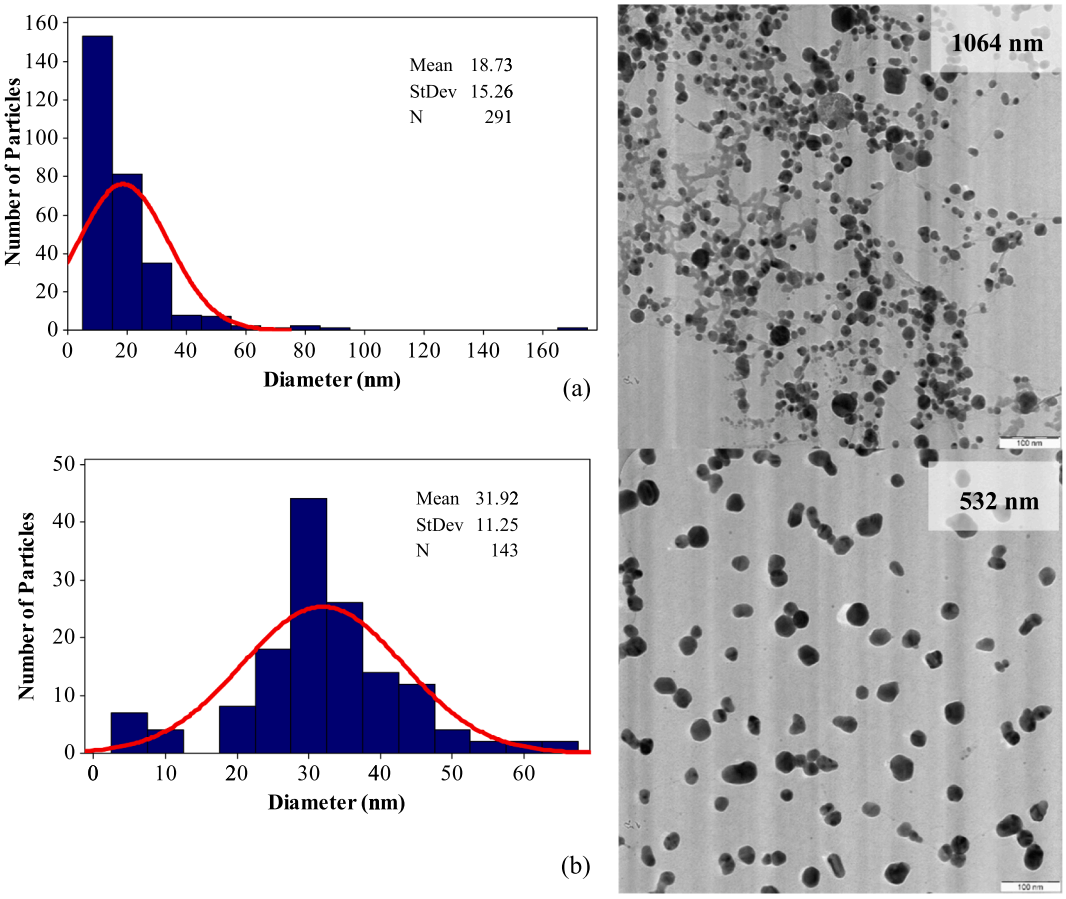

Fig. 6. Histogram of the size distribution and TEM images of the AgNPs produced by (a) 1064 nm and (b) 532 laser wavelengths in distilled water.

Nd:Y3Al5O12). Five different 99.99% purity of metals which are gold (Au), silver (Ag), copper (Cu), aluminium (Al) and nickel (Ni) were used to prepare each of the nanoparticles each with thickness of 0.6 mm, 0.6 mm, 0.1 mm, 1.04 mm and 0.6 mm respectively. To synthesize the nanoparticles, the metals were placed respectively in a 10 ml glass with 3 ml of distilled water as shown in Fig. 1. The laser was operated with two different wavelengths for each metal; 1064 nm which is a near infrared laser and 532 nm which is a green laser with fixed repetition rate frequency of 5 Hz and a total of 1000 laser pulses. The focusing lens with a focal length of 100 mm was used to focus the laser beam on the targets. Four different pulse energies which are 350 mJ, 550 mJ, 750 mJ and 950 mJ were used to ablate the metals.

Characterization of the nanoparticles was done optically by conducting spectroscopy analysis using Ocean Optics QE65000 Spectrometer while morphological and structural characterization were done by using transmission electron microscopy (TEM). The absorbance spectrum of the nanoparticle solutions was recorded immediately after the synthesis was done. These measurements were compared for different laser pulse energy for each respective metals and to be compared to the predicted spectrum based on theory. In this experiment, Zeiss LIBRA® 120 transmission electron microscope was used to acquire images of the nanoparticles. For TEM analysis, only nanoparticles samples from the highest laser pulse energy (i.e. 950 mJ) was observed. The TEM images of the samples were recorded as soon as after the nanoparticles synthesis was completed due to potential rapid growth and aggregation of nanoparticles [16]. Particle size distributions were determined from TEM images by using ImageJ which is an open source Java image processing program by measuring the diameter of nanoparticles from TEM images and the average diameter size is calculated.

Results

Reduction of bulk metal targets into nanoparticles during exposure to laser ablation was observed as a result of colour change as shown in Fig. 2. The colour change is due to the surface plasmon resonance (SPR) phenomenon. The metal nanoparticles have free electrons, which give the SPR absorption band, due to the combined vibration of electron of metal nanoparticles in resonance with light wave. The nanoparticles were characterized in terms of optical and size distribution by spectroscopy absorption and TEM analysis.

Au nanoparticles

Laser ablation of gold target resulted in a purplish-red coloration of water, which is typically attributed to plasmonic excitation effects in the formed AuNPs. The absorption spectra of the synthesized AuNPs at different laser pulse energies using laser wavelength of 1064 nm and

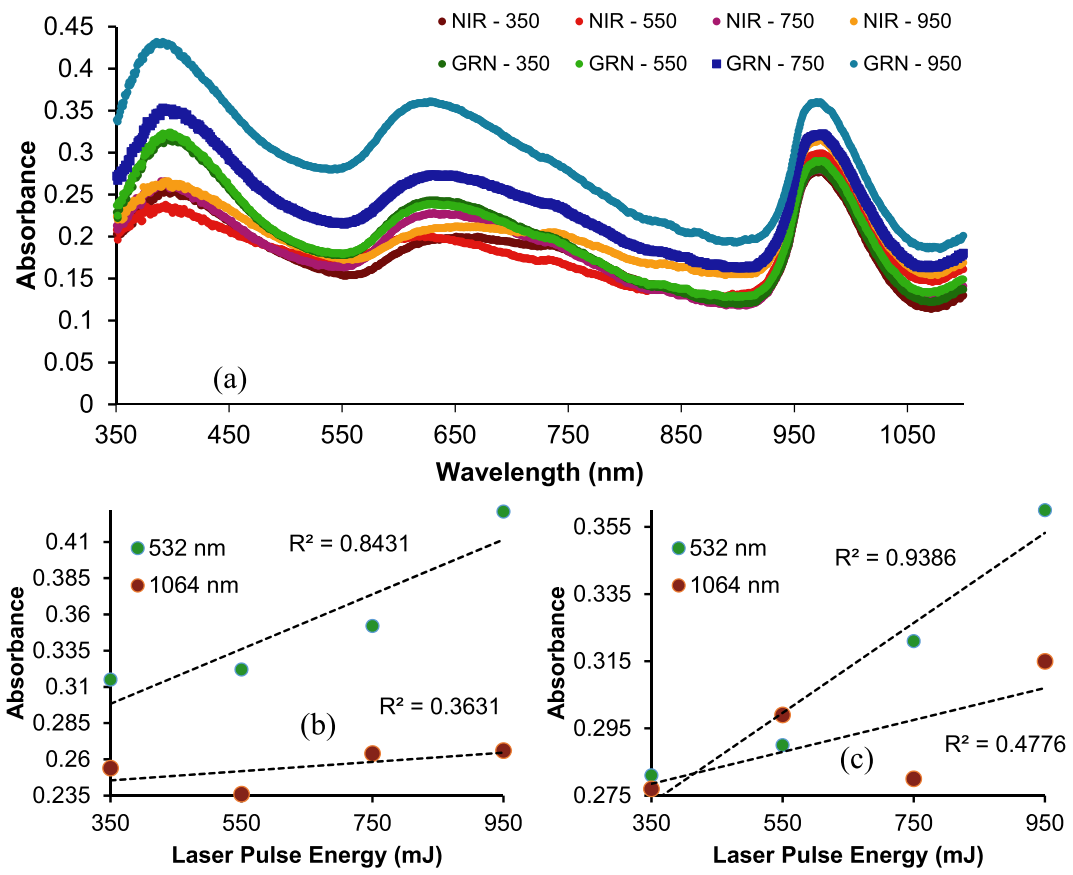

Fig. 7. (a) Absorption spectra of the synthesized CuNPs by different NIR (1064 nm) and green (532 nm) laser energies. Linear regression between absorbance and laser pulse energies measured using (b) peak visible spectra at 396.15 nm and 393.02 nm for CuNPs synthesized by 1064 nm and 532 nm laser respectively and (c) peak NIR spectra at 974.05 nm and 972.6 nm for CuNPs synthesized by 1064 nm and 532 nm laser respectively. (For interpretation of the references to color in this figure legend, the reader is referred to the web version of this article.)

532 nm for ablation are shown in Fig. 3. It is found that the absorption peaks increase with laser pulse energy. A strong absorption peak is observed at the highest laser pulse energy of 950 mJ. Based on the graphs in Fig. 3, two distinctive absorption peaks can be observed in each different electromagnetic spectrum region; visible (VIS) region (380 nm to 700 nm) and near-infrared (NIR) region (above 750 nm). For 1064 nm laser, the peak wavelength of AuNPs in VIS region is 519.81 nm while in NIR region is 974.05 nm. For 532 nm laser, the absorption peak wavelength of AuNPs in VIS region are 518.27 nm while in NIR region is 972.6 nm. The absorption peak wavelengths at approximately 518 nm is consistent with the reported interband transition of Au at 2.4 eV (516 nm) Temple and Bagnall [43]. The peak in NIR region indicate the absorption of distilled water as media Omar et al. [22–23]. Generally, the absorption peak for the AuNPs produced by the 1064 nm laser wavelength is lower than 532 nm laser. The correlation between absorbance and laser pulse energy can be seen in Fig. 2 as the laser pulse energy increases, the spectral absorption by the nanoparticles also increases.

Fig. 4 shows the histogram of size distribution and TEM images of the AuNPs produced by 532 nm and 1064 nm laser in distilled water. The AuNPs produced by 532 nm laser are smaller in compared to nanoparticles produced by 1064 nm, in average measuring 5 nm and 12 nm, respectively. However, it can be noted that there are a few numbers of particles which exceed the nanoscale (> 100 nm). This is due the AuNPs fused into each other as shown in Fig. 3(a). It can be observed that the dispersion of AuNPs generated at the 532 nm are more uniform than those generated at the 1064 nm laser where most of them appeared clustered.

Ag nanoparticles

During ablation of the silver target, the color of solution gradually changed to yellow which indicated the presence of AgNPs. Absorption spectra in visible to near-infrared region of AgNPs prepared by 1064 nm and 532 nm laser ablations at different laser pulse energies are presented in Fig. 5. The absorption peak increases with the laser pulse energy. Besides, from Fig. 4 it can be observed that for 1064 nm and 532 nm laser wavelength, colloidal nanoparticles exhibited a characteristic peak of 417.27 nm and 421.17 nm in VIS region, associated with the excitation of surface plasmon over the nanoparticles. The observed absorption peaks (417.27 nm and 421.17 nm) are lower in energy in comparison to the interband transition energy of Ag at 3.8 eV (326 nm), indicating that the peaks represent intraband transitions Temple and Bagnall [43]. While in NIR region, the absorbance peak wavelength for 1064 nm and 532 nm laser are 972.6 nm and 973.33 nm, respectively. The difference of absorption peak of

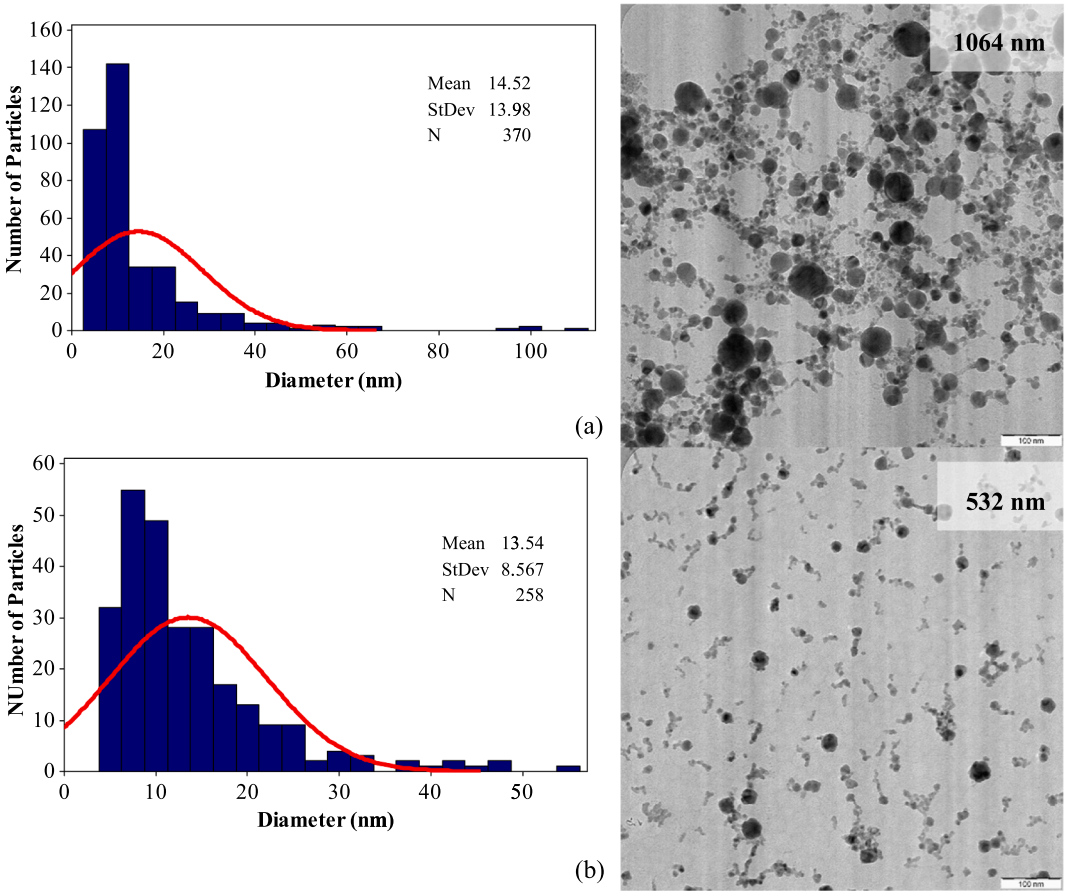

Fig. 8. Histogram of the size distribution and TEM images of the CuNPs produced by (a) 1064 nm and (b) 532 laser wavelengths in distilled water.

nanoparticles ablated by both lasers can be seen wherein the absorption peak intensity for the AgNPs produced by the 1064 nm laser is lower than by 532 nm laser.

The histogram of size distribution and TEM images of AgNPs are shown in Fig. 6. The average size for AuNPs synthesized by 1064 nm and 532 nm lasers is 19 nm and 32 nm, respectively. The average size of AgNPs is larger when produced by 532 nm laser compared to 1064 nm and can be clearly distinguished based on the AgNPs TEM images in Fig. 6. However, the AgNPs synthesized by the 532 nm laser are uniformly dispersed than those synthesized by the 1064 nm laser which appeared to be clustered to each other. Thus, there are a number of nanoparticles that exceed the nanoscale of 100 nm for AuNPs produced by 1064 nm laser. It is noted that some of the AgNPs synthesized by the 532 nm laser are elongated (2–3 particles fused together) and this may be attributed to the laser fluence (up to 950 mJ) with sufficient energy to promote the melting of individual NPs and thereby inducing the formation of interconnected particles [47]. It was also reported previously that unvaporised melts of material may have resolidified forming larger sized particles [29].

Cu nanoparticles

The colloidal CuNPs in distilled water after ablation had a light bluish-green color. Optical absorption spectra of CuNPs in distilled water synthesized by 1064 nm and 532 nm lasers with different pulse energies are shown in Fig. 7. Similar to observation for AuNPs and AgNPs, it can be observed that the absorption peak increases with the laser pulse energy. As can be seen, there are two distinctive peaks for CuNPs within visible region. One appeared within red wavelengths and the other lies towards ultraviolet ends. For 1064 nm laser ablation, the peak within VIS region appeared at 396.15 nm and 650.87 nm while in NIR region at 974.05 nm. On the other hand, for 532 nm laser ablation wavelength, the absorption peak of CuNPs in VIS region is at 393.02 nm and 629.55 nm while in NIR region at 972.6 nm. The absorption peak for the CuNPs produced by the 1064 nm laser is lower than 532 nm laser wavelength. As the reported interband energy threshold for Cu is at 2.1 eV (590 nm) Temple and Bagnall [43], therefore the 396.15 nm and 393.02 nm absorption peaks are interband transitions while 650.87 nm and 69.55 nm peaks are intraband transitions.

The size distribution histograms of CuNPs at 1064 nm and 532 nm laser ablation wavelength are shown in Fig. 7. The average size of the CuNPs synthesized by 1064 nm and 532 nm lasers is 15 nm and 14 nm, respectively. The size distribution of CuNPs imparts that the particles have almost the same average size for both laser wavelengths. Fig. 8 also shows TEM images of CuNPs which were synthesized in distilled water. From these TEM images, it can be seen that CuNPs synthesized by 1064 nm laser have larger particle size than 532 nm. However, despite comparable average particles size, ablation by 532 nm laser did not produce particles larger than 60 nm.

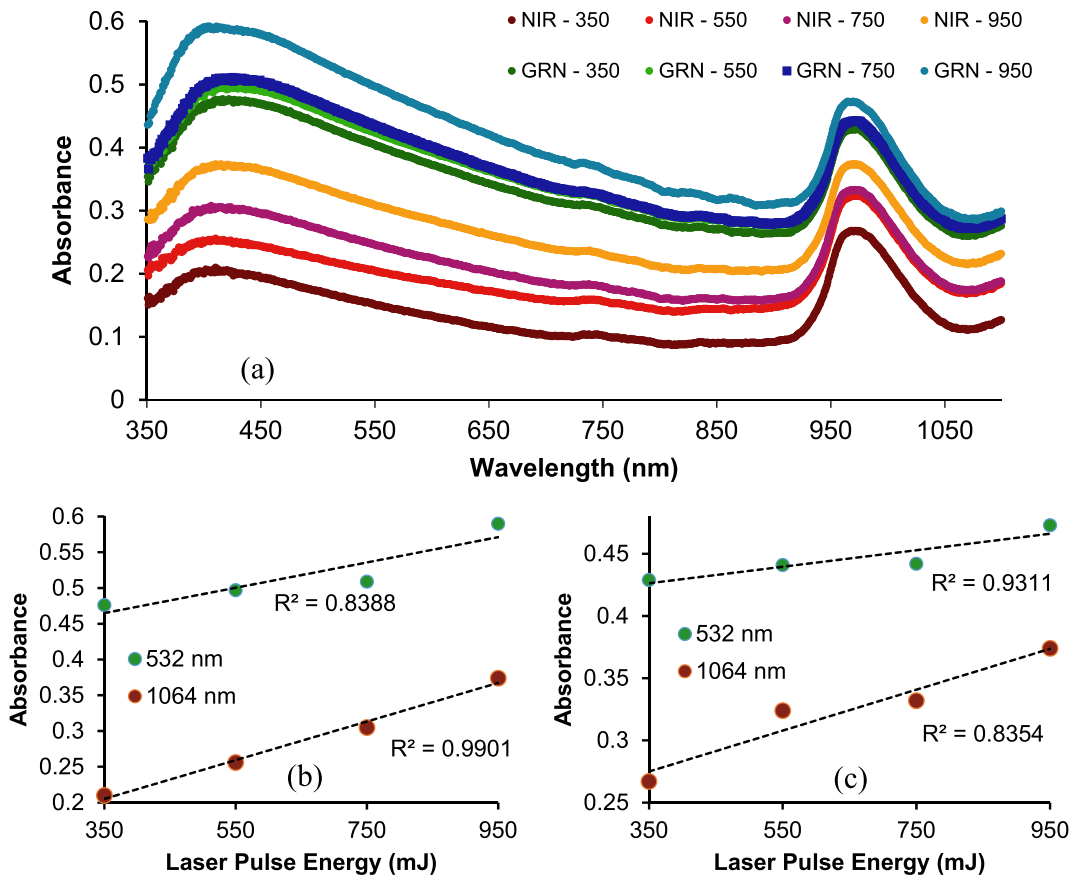

Fig. 9. (a) Absorption spectra of the synthesized AlNPs by different NIR (1064 nm) and green (532 nm) laser energies. Linear regression between absorbance and laser pulse energies measured using (b) peak visible spectra at 410.23 nm for AlNPs synthesized by both 1064 nm and 532 nm laser and (c) peak NIR spectra at 970.43 nm and 969.7 nm for AlNPs synthesized by 1064 nm and 532 nm laser respectively. (For interpretation of the references to color in this figure legend, the reader is referred to the web version of this article.)

Al nanoparticles

The colloidal AlNPs solution in distilled water obtained with laser ablation exhibit a white coloration which turns the solution visually cloudy. Fig. 9 shows absorption spectra of AlNPs in distilled water using two laser wavelengths at different laser pulse energies for ablation. Absorption peaks at 410.23 nm and 970.43 nm is observed for 1064 nm, while for 532 nm, absorption peaks for AlNPs are observed at 410.23 nm and 969.7 nm.

The absorption peak increases with the laser pulse energy. It can be seen that when 1064 nm laser is used for ablation, the peak absorption of AlNPs distinctively less than nanoparticles produced by 532 nm laser. With the Al interband energy threshold being lower at 1.5 eV (825 nm), thus the higher energy absorption peaks near 410 nm are attributed to interband transitions of AlTemple and Bagnall [43].

Fig. 10 shows the histogram of size distribution and TEM images of the AlNPs synthesized by 532 nm and 1064 nm laser wavelengths in distilled water. Well-defined particles with average size of 22 nm and 7 nm were obtained for 1064 nm and 532 nm laser wavelengths, respectively. The average size of AlNPs is larger when produced by 1064 nm laser compared to 532 nm.

Ni nanoparticles

The synthesis of NiNPs in distilled water produced a slight yellow solution. Absorption spectra in VIS to NIR region of NiNPs prepared by 1064 nm and 532 nm laser ablations at different laser pulse energy are presented in Fig. 11. As expected, the absorption peak increases with the laser pulse energy. For 1064 nm laser wavelength, the absorbance peak of NiNPs in VIS region is located at 439.12 nm while in NIR region, it is at 972.6 nm. For 532 nm laser wavelength, the absorption peak of NiNPs in VIS region is at 411.8 nm while in NIR region is at 972.6 nm. The absorption peak for the NiNPs produced by the 1064 nm laser wavelength is slightly lower than at 532 nm laser wavelength. The reported interband energy for Ni is are much higher at 4.7 eV (264 nm) which implies that the observed peaks in the NIR region (411.8 nm and 439.12 nm) in this work are related to intraband transitions.

The size distribution histogram and TEM images of NiNPs are shown in Fig. 12. From the size distribution analysis, the NiNPs have almost the same average size for nanoparticles synthesized by 1064 nm and 532 nm lasers which are 6 nm and 5 nm, respectively. For TEM analysis of NiNPs, it can be stated that the NiNPs produced by both laser wavelength do not exceed the nanoscale of 100 nm. Moreover, the size of NiNPs is very small ranging only between 1 and 25 nm.

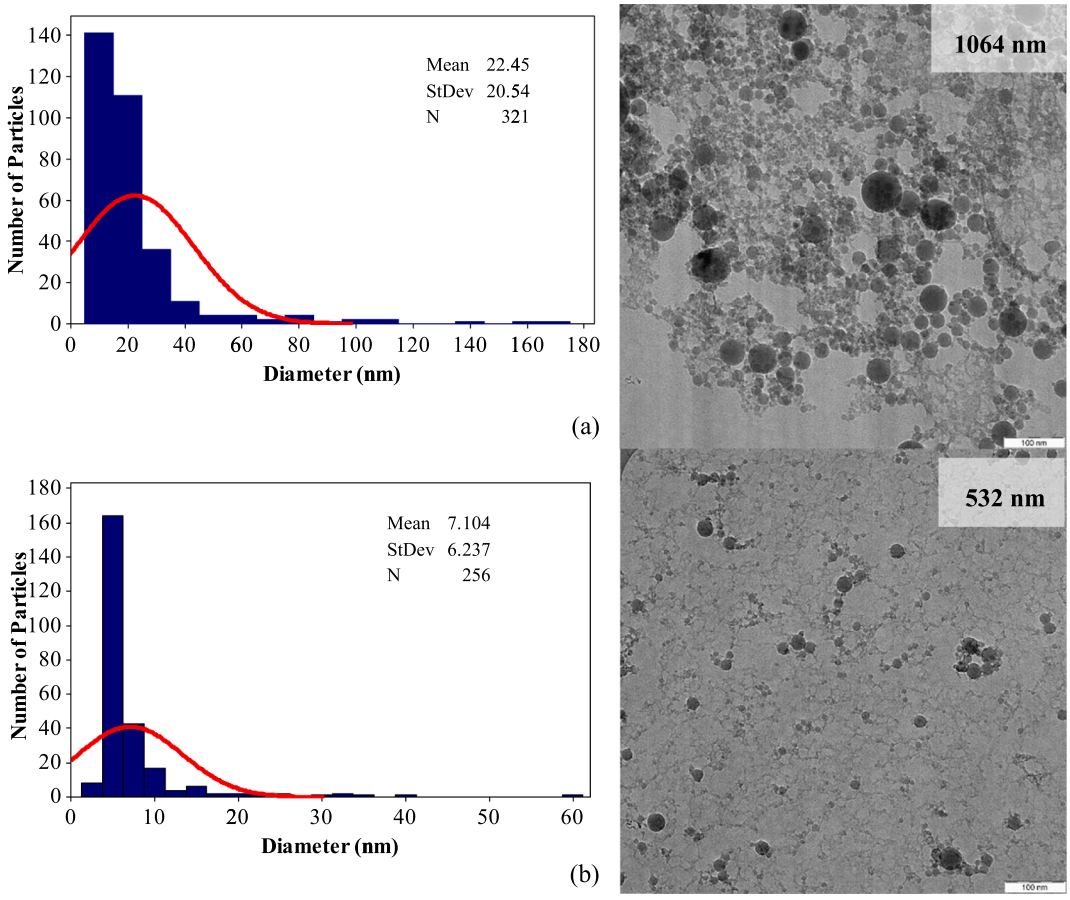

Fig. 10. Histogram of the size distribution and TEM images of the AlNPs produced by (a) 1064 nm and (b) 532 laser wavelengths in distilled water.

Discussion

The synthesis of NPs by pulse laser ablation in distilled water are noticeable by the colour variation of the metal NPs in solution, ranging from colourless to a particular colour for each NPs arising from SPR phenomenon. The effect of laser pulse energies on the absorption peak can be observed wherein the absorption peak of NPs increase with the increase in laser pulse energy. The rise of the absorption peaks can be attributed to the increase of the number of nanoparticles commensurate with higher laser energy provided for ablation.

From the absorption spectrum, two distinct peaks can be observed at the VIS and NIR regions. The observed peaks in the VIS region indicate that the SPR absorption characteristic comprise of distinct wavelengths for each synthesized metal NPs. Conversely, in the NIR region, all the metal NPs under study exhibited common absorption peaks near 970 nm, attributable to water absorption Omar et al. [22,23] being consistent with the fact that all the nanoparticles are suspended in distilled water.

The effects of laser wavelength on absorption intensity was observed; with reducing laser wavelength (higher energy) producing higher absorption intensity. Additionally, metal nanoparticles and metal targets absorb the laser beam energy at particular wavelengths [33]. When NIR wavelength of laser (i.e. 1064 nm) is utilized, the peak absorption intensity of metals nanoparticles is reduced. The ablation efficiency of a metal target decreases with increasing laser wavelength due to the self-absorption of radiation by solvent or generated metal particles in the path of incident laser beam during the ablation [38]. The absorption peak wavelengths for each type of metal nanoparticles is summarized in Table 2.

The absorption peak wavelength of metals nanoparticles within VIS region is the main interest of the spectroscopy analysis. It is because each metal nanoparticles exhibit unique solution color and subsequently spectral pattern with distinctive peak VIS absorbance wavelength in relation to SPR. Though NIR wavelengths is commonly associated with the measurement of particles in water due to its strong immunity towards different colored particles [24,55]. The absorption peak wavelength of AuNPs, AgNPs and CuNPs in VIS region are in agreement with the previous studies by Amendola and Meneghetti [2] while for AlNPs and NiNPs, the previous studies by Singh and Soni [38] also Shalichah and Khumaeni [36] showed different result of the absorption peak wavelength. This might due to oxidation in AlNPs and NiNPs. The fast hydrolysis reaction between Al and water altered the composition of AlNPs to Al oxides in the absence of surfactant and with ageing. The oxidation of CuNPs also can occur but it consumes more time up to two weeks after the ablation to oxidize [44].

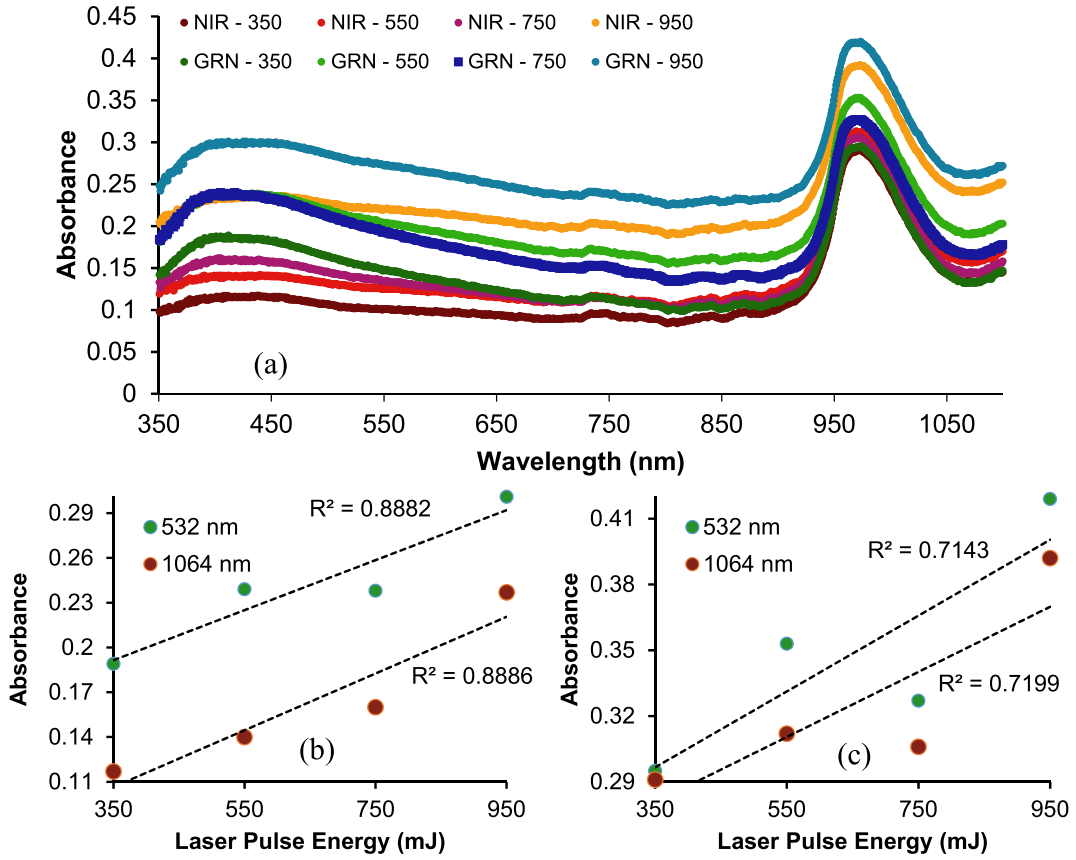

Fig. 11. (a) Absorption spectra of the synthesized NiNPs by different NIR (1064 nm) and green (532 nm) laser energies. Linear regression between absorbance and laser pulse energies measured using (b) peak visible spectra at 439.12 nm and 411.8 nm for NiNPs synthesized by 1064 nm and 532 nm laser respectively and (c) peak NIR spectra at 972.6 nm for NiNPs synthesized by both 1064 nm and 532 nm laser. (For interpretation of the references to color in this figure legend, the reader is referred to the web version of this article.)

For this experiment, colorimetric interpretation of synthesized nanoparticles manages to provide better relationship or higher correlation coefficient, R between absorbance and laser energy ablated to the metal plate. Higher laser energy ablated to the metal plates synthesizes higher concentration of nanoparticles [1,16]. For TEM analysis, the size distribution of NPs can be determined. The sizes of nanoparticles produced are within the nanoscale range of 1 to 100 nm. Nevertheless, there are still a small number of nanoparticles which exceed the nanoscale (> 100 nm) especially for nanoparticles produced by 1064 nm laser. This is due to the fusion and agglomeration of the nanoparticles which leads to larger particle size interpretation during size distribution analysis using ImageJ software. The average size of nanoparticles for both laser wavelengths is summarized in Table 3.

From Table 3, it can be concluded that significantly smaller AuNPs and AlNPs were synthesized by 532 nm laser, while smaller AgNPs were synthesized by 1064 nm laser. There is no noticeable difference in the size of the CuNPs and NiNPs synthesized by 532 and 1064 nm lasers. Different laser wavelengths also resulted in different responses to energy loss within the water located above the target materials. Thus, different size of the nanoparticles would be formed, if the energy loss was not corrected [9]. Also, the average size of NiNPs is the smallest compared to the others which might due to the hardness of the metals as the Mohs scale of hardness of nickel is 4 while Au, Ag, Cu, and Al are 2.5–3 [34].

Conclusion

In this study, Au, Ag, Cu, Al and Ni nanoparticles were successfully synthesized by pulse laser ablation in distilled water using laser wavelengths of 1064 nm and 532 nm. The effect of laser pulse energy and laser wavelength on the absorption spectra and size distribution for different metal nanoparticles were studied. The absorption peak intensity of investigated NPs was found to be dependent on the laser pulse energy whereby as the laser pulse energy increase, the absorption peak of resulting nanoparticles increases. In addition, higher absorption peak can be observed for the shorter laser wavelength of 532 nm compared to 1064 nm. Additionally, the wavelength of laser affects the size of the nanoparticles. For 1064 nm laser, smaller AgNPs were synthesized while for 532 nm, smaller AuNPs and AlNPs were produced. However, for CuNPs and NiNPs the size of nanoparticles produced were almost similar for both wavelengths. From TEM analysis, it can be stated that the synthesized nanoparticles were spherical in shape with sizes within the 1 nm to 100 nm range except for some nanoparticles which appeared to have agglomerated.

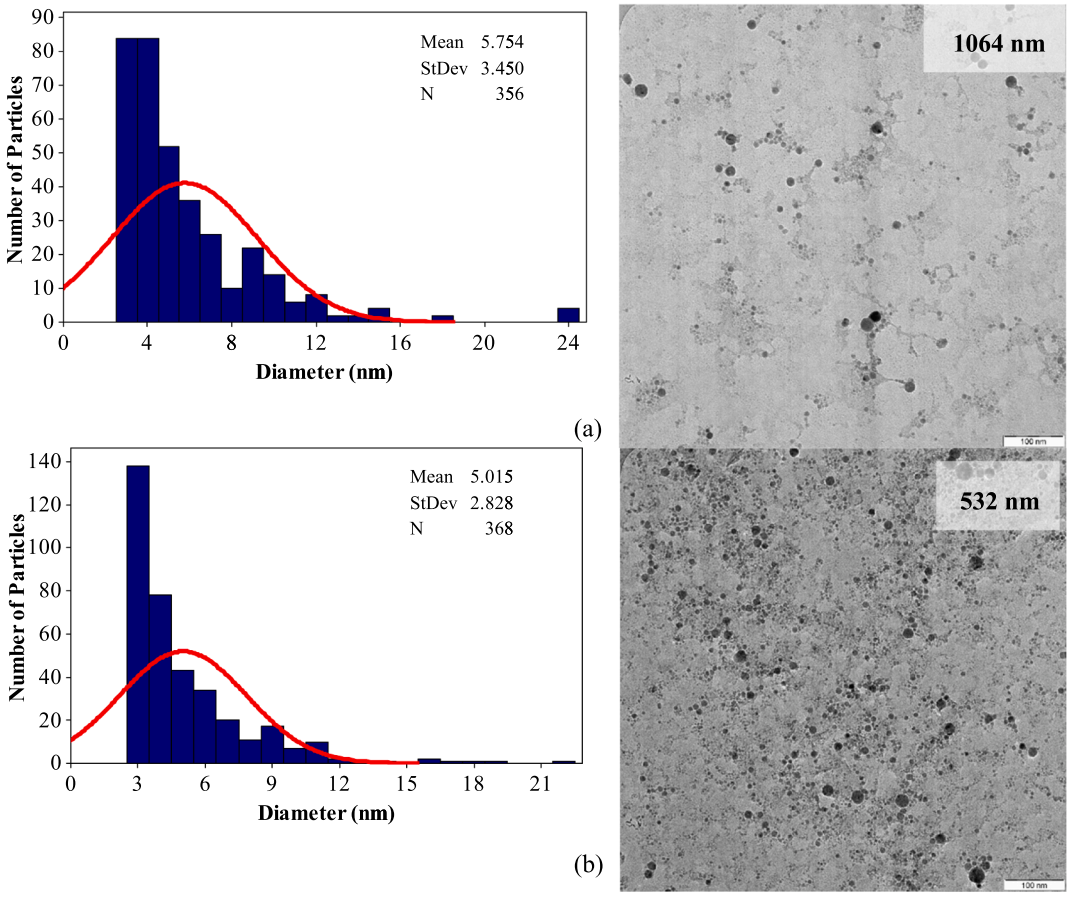

Fig. 12. Histogram of the size distribution and TEM images of the NiNPs produced by (a) 1064 nm and (b) 532 laser wavelengths in distilled water.

Table 2
Absorption peak wavelength for each nanoparticle type and laser synthesis.

Type of nanoparticles	(a) Absorption peak wavelength (nm) at 1064 nm laser		(b) Absorption peak wavelength (nm) at 532 nm laser	
	VIS region	NIR region	VIS region	NIR region
AuNPs	519.81	974.05	518.27	972.6
AgNPs	417.27	972.6	421.17	973.33
CuNPs	396.15/ 650.87	974.05	393.02/ 629.55	972.6
AlNPs	410.23	970.43	410.23	969.7
NiNPs	411.02	972.6	411.8	972.6

Table 3
Analysis of the particle size distribution.

Type of nanoparticles	Average diameter size (nm)	
	Infrared laser (1064 nm)	Green laser (532 nm)
AuNPs	12	5
AgNPs	19	32
CuNPs	15	14
AlNPs	22	7
NiNPs	6	5

References

[1] Abdulateef SA, Omar AF, Jafri MM, Ahmed NM, Seeni A. One-step synthesis of stable colloidal gold nanoparticles through bioconjugation with bovine serum albumin in harsh environments. J Cluster Sci 2017;28(6):3193–207.

[2] Amendola V, Meneghetti M. Laser ablation synthesis in solution and size manipulation of noble metal nanoparticles. PCCP 2009;11(20):3805–21.

[3] Baladi A, Mamoory RS. Study on wavelength and energy effects on pulsed laser ablation synthesis of aluminum nanoparticles in ethanol. MEMS, NANO, and Smart Systems (ICMENS). 2009 Fifth International Conference. IEEE; 2009. p. 218–21.

[4] Baladi A, Mamoory RS. Investigation of different liquid media and ablation times on pulsed laser ablation synthesis of aluminum nanoparticles. Appl Surf Sci 2010;256(24):7559–64.

[5] Baruah PK, Singh A, Rangan L, Sharma AK, Khare A. Optimization of copper nanoparticles synthesized by pulsed laser ablation in distilled water as a viable SERS substrate for karanjin. Mater Chem Phys 2018.

[6] Boutinguiza M, Comesaña R, Lusquiños F, Riveiro A, Del Val J, Pou J. Production of silver nanoparticles by laser ablation in open air. Appl Surf Sci 2015;336:108–11.

[7] Fu GS, Wang YL, Chu LZ, Zhou Y, Yu W, Han L, et al. The size distribution of Si nanoparticles prepared by pulsed-laser ablation in pure He, Ar or Ne gas. Europhys Lett 2005;69(5):758.

[8] Habieb AA, Soary AO, Mmohammed KA. Effect of laser wavelength on the fabrication of gold nanoparticles by laser ablation. Int J Res Appl Nat Soc Sci 2016:125–30.

[9] Hamad A, Li L, Liu Z. Comparison of characteristics of selected metallic and metal oxide nanoparticles produced by picosecond laser ablation at 532 and 1064 nm wavelengths. Appl Phys A 2016;122(10):904.

[10] Kazemizadeh F, Malekfar R, Parvin P. Pulsed laser ablation synthesis of carbon nanoparticles in vacuum. J Phys Chem Solids 2017;104:252–6.

[11] Kuladeep R, Jyothi L, Prakash P, Mayank Shekhar S, Durga Prasad M, Narayana Rao D. Investigation of optical limiting properties of Aluminium nanoparticles prepared by pulsed laser ablation in different carrier media. J Appl Phys 2013;114(24):243101.

[12] Lasemi N, Pacher U, Zhigilei LV, Bomatí-Miguel O, Lahoz R, Kautek W. Pulsed laser ablation and incubation of nickel, iron and tungsten in liquids and air. Appl Surf Sci 2018;433:772–9.

[13] Liu P, Wang H, Li X, Rui M, Zeng H. Localized surface plasmon resonance of Cu nanoparticles by laser ablation in liquid media. RSC Adv 2015;5(97):79738–45.

[14] Mansoureh G, Parisa V. Synthesis of metal nanoparticles using laser ablation technique. Emerging Applications of Nanoparticles and Architecture Nanostructures. Elsevier; 2018. p. 575–96.

[15] Mardis M, Takada N, Machmudah S, Sasaki K, Kanda H, Goto M. Nickel nanoparticles generated by pulsed laser ablation in liquid CO 2. Res Chem Intermed 2016;42(5):4581–90.

[16] Moura CG, Pereira RSF, Andritschky M, Lopes ALB, de Freitas Grilo JP, do

Nascimento RM, Silva FS. Effects of laser fluence and liquid media on preparation of small Ag nanoparticles by laser ablation in liquid. Opt Laser Technol 2017;97:20–8.
[17] Muñetón Arboleda D, Santillán JM, Mendoza Herrera LJ, van Raap MBF, Mendoza Zélis P, Muraca D, et al. Synthesis of Ni nanoparticles by femtosecond laser ablation in liquids: structure and sizing. J Phys Chem C 2015;119(23):13184–93.
[18] Muniz-Miranda M, Gellini C, Simonelli A, Tiberi M, Giammanco F, Giorgetti E. Characterization of copper nanoparticles obtained by laser ablation in liquids. Appl Phys A 2013;110(4):829–33.
[19] Nagarajan R. Nanoparticles: building blocks for nanotechnology. Nanoparticles: synthesis, stabilization, passivation, and functionalization. 2008. p. 2–14.
[20] Nikov RG, Nedyalkov NN, Nikolov AS, Atanasov PA, Alexandrov MT, Karashanova DB. Formation of bimetallic nanoparticles by pulsed laser ablation of multi-component thin films in water. 18th International School on. Quant Electron: Laser Phys Appl 2015;9447:94470M.
[21] Oliveira E, Núñez C, Santos HM, Fernández-Lodeiro J, Fernández-Lodeiro A, Capelo JL, et al. Revisiting the use of gold and silver functionalised nanoparticles as colorimetric and fluorometric chemosensors for metal ions. Sens Actuators B 2015;212:297–328.
[22] Omar AF, Atan H, MatJafri MZ. NIR spectroscopic properties of aqueous acids solutions. Molecules 2012;17(6):7440–50.
[23] Omar AF, Atan H, MatJafri MZ. Peak response identification through near- infrared spectroscopy analysis on aqueous sucrose, glucose, and fructose solution. Spectrosc Lett 2012;45(3):190–201.
[24] Omar AF, MatJafri MZ. Development of optical instrument as turbidimeter: a comparative study. Sens Rev 2012;32(2):134–41.
[25] Palazzo G, Valenza G, Dell'Aglio M, De Giacomo A. On the stability of gold nanoparticles synthesized by laser ablation in liquids. J Colloid Interface Sci 2017;489:47–56.
[26] Patra N, Patil R, Sharma A, Singh V, Palani IA. Comparative study on Cu, Al and Cu-Al alloy nanoparticles synthesized through underwater laser ablation technique. IOP conference series: materials science and engineering. IOP Publishing; 2018. p. 012046. No. 1.
[27] Piriyawong V, Thongpool V, Asanithi P, Limsuwan P. Effect of laser pulse energy on the formation of alumina nanoparticles synthesized by laser ablation in water. Procedia Eng 2012;32:1107–12.
[28] Priyadarshini E, Pradhan N. Gold nanoparticles as efficient sensors in colorimetric detection of toxic metal ions: a review. Sens Actuators B 2017;238:888–902.
[29] Rawat R, Tiwari A, Vendamani VS, Pathak AP, Rao SV, Tripathi A. Synthesis of Si/SiO2 nanoparticles using nanosecond laser ablation of silicate-rich garnet in water. Opt Mater 2018;75:350–6.
[30] Reich S, Schönfeld P, Wagener P, Letzel A, Ibrahimkutty S, Gökce B, et al. Pulsed laser ablation in liquids: impact of the bubble dynamics on particle formation. J Colloid Interface Sci 2017;489:106–13.
[31] Resano-Garcia A, Battie Y, Koch A, En Naciri A, Chaoui N. Influence of the laser light absorption by the colloid on the properties of silver nanoparticles produced by laser ablation in stirred and stationary liquid. J Appl Phys 2015;117(11):113103.
[32] Sadrolhosseini AR, Abdul Rashid S, Zakaria A, Shameli K. Green fabrication of copper nanoparticles dispersed in walnut oil using laser ablation technique. J Nanomater 2016;2016:62.
[33] Sadrolhosseini AR, Mahdi MA, Alizadeh F, Rashid SA. Laser ablation technique for synthesis of metal nanoparticle in liquid. Laser technology and its applications. IntechOpen; 2018.
[34] Samsonov GV. Mechanical properties of the elements. In: Samsonov GV, editor. Handbook of the physicochemical properties of the elements. Boston, MA: Springer; 1968. p. 432.
[35] Scaramuzza S, Zerbetto M, Amendola V. Synthesis of gold nanoparticles in liquid environment by laser ablation with geometrically confined configurations: insights to improve size control and productivity. J Phys Chem C 2016;120(17):9453–63.
[36] Shalichah C, Khumaeni A. Synthesis of nickel nanoparticles by pulse laser ablation method using Nd: YAG laser. J Phys: Conf Ser 2018;1025(1):12002. IOP Publishing.
[37] Shukri WN, Bidin N, Affandi S, Bohari SP. Synthesize of gold nanoparticles with 532 nm and 1064 nm pulsed laser ablation. J Teknologi 2015;78(3):267–70.
[38] Singh R, Soni RK. Laser synthesis of aluminium nanoparticles in biocompatible polymer solutions. Appl Phys A 2014;116(2):689–701.
[39] Solati E, Mashayekh M, Dorranian D. Effects of laser pulse wavelength and laser fluence on the characteristics of silver nanoparticle generated by laser ablation. Appl Phys A 2013;112(3):689–94.
[40] Stratakis E, Barberoglou M, Fotakis C, Viau G, Garcia C, Shafeev GA. Generation of Al nanoparticles via ablation of bulk Al in liquids with short laser pulses. Opt Express 2009;17(15):12650–9.
[41] Svetlichnyi VA, Shabalina AV, Lapin IN, Goncharova DA. Metal oxide nanoparticle preparation by pulsed laser ablation of metallic targets in liquid. Applications of laser ablation-thin film deposition, nanomaterial synthesis and surface modification. IntechOpen; 2016.
[42] Swarnkar RK, Singh SC, Gopal R. Effect of aging on copper nanoparticles synthesized by pulsed laser ablation in water: structural and optical characterizations. Bull Mater Sci 2011;34(7):1363–9.
[43] Temple TL, Bagnall DM. Optical properties of gold and aluminium nanoparticles for silicon solar cell applications. J Appl Phys 2011;109(8):084343.
[44] Tilaki RM, Mahdavi SM. Size, composition and optical properties of copper nanoparticles prepared by laser ablation in liquids. Appl Phys A 2007;88(2):415–9.
[45] Tomko J, Naddeo JJ, Jimenez R, Tan Y, Steiner M, Fitz-Gerald JM, et al. Size and polydispersity trends found in gold nanoparticles synthesized by laser ablation in liquids. Phys Chem Chem Phys 2015;17(25):16327–33.
[46] Tsai SH, Liu YH, Wu PL, Yeh CS. Preparation of Au–Ag–Pd trimetallic nanoparticles and their application as catalysts. J Mater Chem 2003;13(5):978–80.
[47] Vendamani VS, Tripathi A, Pathak AP, Rao SV, Tiwari A. Laser ablation of natural micas: synthesis of MgO and Mg(OH)2 nanoparticles and nanochains. Mater Lett 2017;192:29–32.
[48] Viau G, Collière V, Lacroix LM, Shafeev GA. Internal structure of Al hollow nanoparticles generated by laser ablation in liquid ethanol. Chem Phys Lett 2011;501(4–6):419–22.
[49] Vilela D, González MC, Escarpa A. Sensing colorimetric approaches based on gold and silver nanoparticles aggregation: chemical creativity behind the assay. A review. Anal Chim Acta 2012;751:24–43.
[50] Wagener P, Schwenke A, Barcikowski S. How citrate ligands affect nanoparticle adsorption to microparticle supports. Langmuir 2012;28(14):6132–40.
[51] Wang EC, Wang AZ. Nanoparticles and their applications in cell and molecular biology. Integr Biol 2014;6(1):9–26.
[52] Wojcieszak R, Genet MJ, Eloy P, Ruiz P, Gaigneaux EM. Determination of the size of supported Pd nanoparticles by X-ray photoelectron spectroscopy. J Phys Chem C 2010;114(39):16677–84.
[53] Zamiri R, Azmi BZ, Ahangar HA, Zamiri G, Husin MS, Wahab ZA. Preparation and characterization of silver nanoparticles in natural polymers using laser ablation. Bull Mater Sci 2012;35(5):727–31.
[54] Zhang J, Claverie J, Chaker M, Ma D. Colloidal metal nanoparticles prepared by laser ablation and their applications. ChemPhysChem 2017;18(9):986–1006.
[55] Zhang Q, Zheng L, Mi X, Zhang Y, Li M. Development of a Portable water turbidimeter based on NIR spectroscopy. Sens Transducers 2014;26:75.